Parameter Precision in Global Analysis of Time-Resolved Spectra

Ivo H. M. van Stokkum

***Abstract*— By means of simulation parameter estimation in global analysis of time resolved spectra was studied. Kinetic, spectral as well as spectrotemporal models were used to describe a system consisting of an inherent mixture of components whose concentrations change with time. With a single component the parameter precision did not differ between the different model types. With two or more components the precision decreases with a kinetic or spectral model because of overlap between concentration profiles or spectra of the components. However, with a spectrotemporal model the decrease is much less, and equals zero with zero spectral overlap.**

***Index Terms*— Curve fitting, least-squares methods, modeling, optical spectroscopy, parameter estimation, simulation, system identification.**

I. Introduction

THE KINETIC and spectral properties of a system consisting of an inherent mixture of components whose concentrations change with time can be studied by means of time-resolved spectroscopy. To identify such a system, the parameters which describe the kinetics and spectra of the components have to be estimated. Overlap of the concentration profiles or spectra of the components complicates this parameter estimation. In the field of molecular photophysics and photochemistry, transient absorption and fluorescence spectroscopy, following an appropriately short exciting pulse of radiation, are widely used [1]–[8] on timescales of picoseconds to seconds. The (impulse) response of the system across wavelength and time results in a so-called time resolved spectrum. According to the Beer–Lambert law the spectroscopic properties of a mixture of components are a superposition of the spectroscopic properties of the components weighted by their concentration. Thus the perfect, noise-free, time-resolved spectrum ψ is a superposition of the contributions of the n_{comp} different components

$$\psi(t,\lambda) = \sum_{l=1}^{n_{\mathrm{comp}}} c_l(t)\varepsilon_l(\lambda) \tag{1}$$

where $c_l(t)$ and $\varepsilon_l(\lambda)$ denote, respectively, the concentration and spectrum of component l. Typically, the number of components studied with time-resolved spectroscopy is less than ten, whereas the number of different wavelengths or the number of different time instants goes up to thousands. Note that according to (1) a separability of time and wavelength properties is possible for each component. Using a physicochemical parametric model, the data are analyzed globally, i.e. with a single model describing the data at all times and wavelengths, in order to improve the parameter precision, e.g. [1]–[8]. We have used kinetic and spectral, as well as spectrotemporal models [3], [8]. The aim of this paper is to study by means of simulation parameter estimation in these three types of models, in particular to investigate the potential benefits of using a more complicated, spectrotemporal model.

Manuscript received June 3, 1996.

The author is with the Faculty of Physics and Astronomy, Vrije Universiteit, 1081 HV Amsterdam, The Netherlands (e-mail: ivo@nat.vu.nl).

Publisher Item Identifier S 0018-9456(97)06464-4.

II. Methods

The basic model which describes the time evolution of spectra is[1]

$$\underline{\psi}_{t_i\lambda_j} = \sum_{l=1}^{n_{\mathrm{comp}}} c_{lt_i}\varepsilon_{l\lambda_j} + \underline{\xi}_{t_i\lambda_j} \tag{2}$$

$$\underline{\Psi} = CE^T + \underline{\Xi} \tag{3}$$

where the $m \times n$ matrix Ψ (with elements $\underline{\psi}_{t_i\lambda_j}$) denotes the time-resolved spectra, measured at m time instants t_i, and n wavelengths λ_j. c_{lt_i} denotes the concentration of component l at time t_i, $\varepsilon_{l\lambda_j}$ denotes the spectrum of component l at wavelength λ_j, and $\underline{\xi}_{t_i\lambda_j}$ denotes a Gaussian distributed stochastic disturbance with zero mean and variance σ^2. The c_{lt_i} and $\varepsilon_{l\lambda_j}$ are stored in the matrices C and E, of dimension $m \times n_{\mathrm{comp}}$ and $n \times n_{\mathrm{comp}}$, respectively. Matrix Ξ is, like Ψ, $m \times n$. Now, three types of model are distinguished.

A. Kinetic Model

The concentrations are described by a kinetic model, which depends upon the nonlinear parameters θ_K, whereas the spectral parameters of the $n \times n_{\mathrm{comp}}$ matrix E are conditionally linear parameters [9], [10]

$$\underline{\Psi} = C(\theta_K)E^T + \underline{\Xi}. \tag{4}$$

B. Spectral Model

The spectra are described by a parametric model, which depends upon the nonlinear parameters θ_S, whereas the concentration parameters of the $m \times n_{\mathrm{comp}}$ matrix C are conditionally linear parameters

$$\underline{\Psi}^T = E(\theta_S)C^T + \underline{\Xi}^T. \tag{5}$$

[1]Notation convention: underlining indicates stochastic variables, uppercase represents matrices, lowercase represents scalars or vectors.

Furthermore, the estimated matrices E from (4) and C from (5) can subsequently be fitted with, respectively, a spectral and a kinetic model.

C. Spectrotemporal Model

Both the concentrations and the spectra are described by a model, which depends upon the nonlinear parameters θ_K and θ_S. Assuming first-order kinetics, a matrix of linear parameters A describes the concentrations of the components in terms of a superposition of simple exponential decays which are stored in the matrix $C(\theta_K)$

$$\underline{\Psi} = C(\theta_K)AE^T(\theta_S) + \underline{\Xi}. \tag{6}$$

With components which decay independently, the matrix A becomes a diagonal matrix $\mathrm{diag}(a)$.

D. Parameter Estimation

The conditionally linear parameters [E in (4), C in (5), A in (6)] can be eliminated in the nonlinear least squares (NLLS) fit by means of the variable projection method [10]–[13]. This is especially profitable when their number is large, e.g., in time-gated spectra analyzed with a kinetic model [3], [7]. The optimization routine uses a modified Levenberg–Marquardt method with a trust region approach [14]. Variable projection was used to calculate the residuals [13], [14], using the Kaufman approximation for their derivatives [10], [11]. As initial values the true values of the parameters were chosen. The precision of the estimated parameters is summarized by the covariance matrix. The linear approximation covariance matrix of the nonlinear parameters θ is estimated from

$$\mathrm{cov}(\hat{\underline{\theta}}) = \hat{\underline{\sigma}}^2(J^TJ)^{-1} \tag{7}$$

where $\hat{\underline{\sigma}}^2$ denotes the estimated variance and J is the Jacobian of the model function with respect to the parameters θ, evaluated at the NLLS estimate $\hat{\underline{\theta}}$. The Kaufman approximation [10], [11] was used to calculate this Jacobian. The linear approximation covariance matrix of the conditionally linear parameters was estimated according to [13].

E. Simulation

Models with one, two, or three components were simulated. The case $n_{\mathrm{comp}} = 2$, which is the first nontrivial case and which is of great practical importance [3], [7], [8], was studied in depth. The concentrations of the components are described by exponential decays $\exp(-kt)$ with rate parameter k, whereas the spectral shapes are described by a Gaussian in the energy domain ($\bar{\nu} = \lambda^{-1}$) [7]

$$\varepsilon(\bar{\nu}) = \bar{\nu}^5 \exp(-\ln 2[2(\bar{\nu} - \bar{\nu}_{\max})/\Delta\bar{\nu}]^2) \tag{8}$$

with parameters $\bar{\nu}_{\max}$, $\Delta\bar{\nu}$ for, respectively, location and full-width-at-half-maximum (FWHM). Thus the simulated data are a function of eight parameters—for each component four parameters: k, $\bar{\nu}_{\max}$, $\Delta\bar{\nu}$, and amplitude a.

The time resolved spectrum was simulated at $m = 51$ time points equidistant in the interval 0–2 ns and $n = 51$ wavelengths equidistant in the interval 350–550 nm. The overlap between the spectra and concentration profiles of the components could be large (EL, CL) or small (ES, CS). The nonlinear parameters of the combinations used in the simulations, whose values are inspired by experimental data [3], [7], [8], are summarized in Table I. Normally distributed noise was added to the simulated data. With the low noise level the standard deviation σ of the noise was equal to 6×10^{-3} of the maximum of the data (CS, ES and CS, EL case) or 3×10^{-3} (CL, ES and CL, EL cases). The high noise level was ten times higher.

TABLE I
PARAMETERS k (IN 10^9 S-1), $\bar{\nu}_{\max}$, $\Delta\bar{\nu}$ (IN 10^3 cm $^{-1}$) AND a OF COMPONENTS

Overlap	CSmall (CS)	CLarge (CL)
ESmall (ES)	0.25, 22, 9, 1	0.5, 22, 9, 1
	1.0, 18, 8, 2	0.6, 18, 8, 2
ELarge (EL)	0.25, 19, 9, 1	0.5, 19, 9, 1
	1.0, 18, 8, 2	0.6, 18, 8, 2

In order to compare the parameter precision with different types of model an ensemble of datasets was simulated with certain parameters and noise level. The deviation $\mathrm{dev}(\theta) = \hat{\underline{\theta}} - \theta$, the difference between the estimated and true value of a parameter, the linear approximation standard error from (7) and the ratio of these two, which is the studentized parameter [9], [16], were calculated. From this ensemble of realizations the rms value was calculated and a smoothed probability density was estimated using the Splus function *ksmooth* [15].

III. RESULTS

The parameter precision was studied as a function of the type of model and of the noise level. With a single component the parameter precision did not differ between the different model types, irrespective of the noise level used. This is due to the complete separability of the time and wavelength properties with a single component (1). With two components, different combinations of overlap of the components were studied. A typical example of a global analysis with the help of a kinetic model of a CL, ES combination data set with low noise is shown in Fig. 1. Note that the fitted curves (dashed lines in Fig. 1(a) and (b) are close to the simulated curves (solid lines). Fig. 2 shows the distributions for k_1 estimated from an ensemble of realizations of this kinetic model fit. The distribution [Fig. 2(a)] of deviation shows no signs of bias (peaking at zero deviation) but it appears a bit skewed. The studentized parameter distribution [Fig. 2(c)] deviates somewhat from a t_{df} distribution which would apply when the model is linear. The improvement gained with a spectrotemporal model is clearly visible in Fig. 3 (note the differences in scale). Note that here the studentized parameter is more closely distributed as t_{df} [Fig. 3(c)] which indicates that the spectrotemporal model is functionally linear [16]. Thus overlap combinations were studied at two noise levels. The averaged results for the two rate constants are collated in Table II. With CS, EL overlap the spectrotemporal model (column ST) provides only a small improvement over the kinetic model (column K). However, with small spectral overlap (CL, ES and CS, ES)

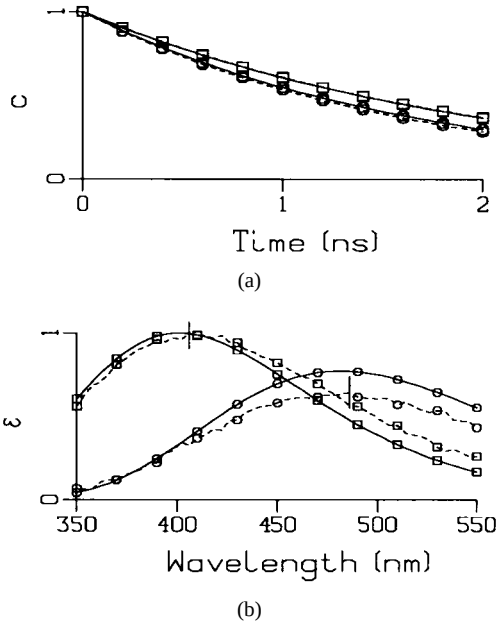

Fig. 1. Global analysis with the help of a kinetic model of CL, ES combination data set with low noise. (a) Concentration profiles. Squares and circles indicate first and second component, respectively. Solid and dashed lines indicate true and fitted, respectively. (b) Spectra, vertical bars indicate plus or minus standard error.

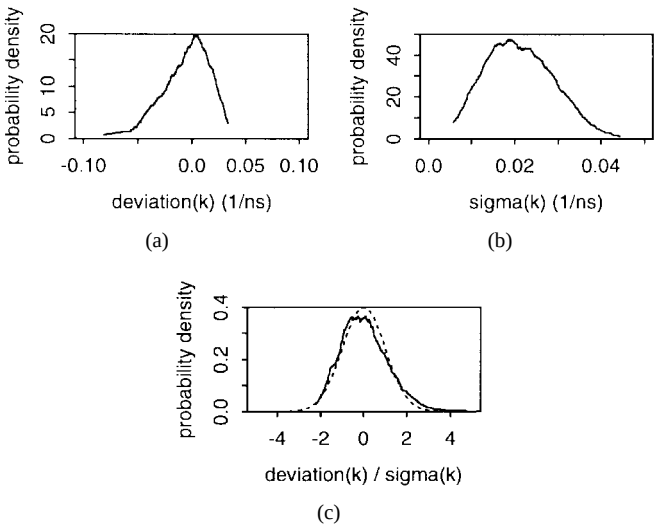

Fig. 2. Distributions estimated from kinetic fit of CL, ES combination with low noise. (a) Deviation of estimated rate constant k_1, (b) standard error, (c) studentized parameter (solid) and t_{df} distribution (dotted).

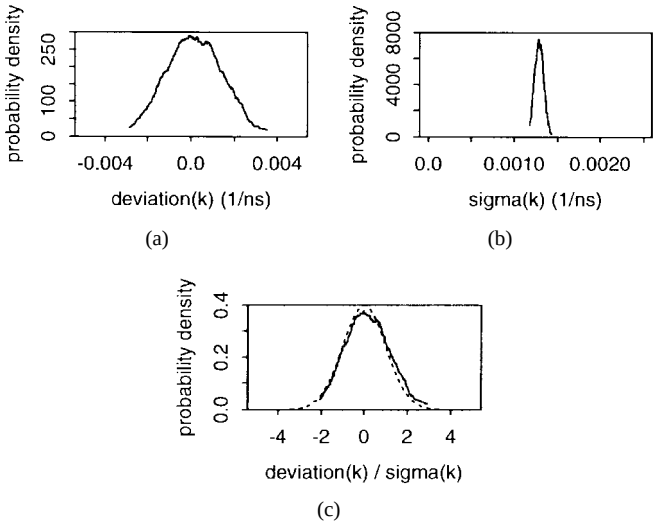

Fig. 3. Distributions estimated from spectrotemporal fit of CL, ES combination with low noise. (a) Deviation of estimated rate constant k_1, (b) standard error, (c) studentized parameter (solid) and t_{df} distribution (dotted).

the spectrotemporal model is clearly superior (compare the K and ST columns of Table II), the precision is increased about tenfold (CL, ES) and twofold (CS, ES). Surprisingly, with CL, EL overlap (and low noise) the spectrotemporal model increased the precision about fivefold. With high noise the kinetic model could no longer resolve two components, which is indicated by the rms deviations being larger than the parameter values (Table I). With the spectrotemporal model the precision was close to the CS, EL overlap, where the noise was two times larger, indicating a tradeoff between (temporal) overlap and noise level. With the spectral parameters the results (not shown) are analogous. With CL, ES overlap the spectrotemporal model provides only a small improvement over the spectral model. However, with small temporal overlap (CS, EL and CS, ES) the spectrotemporal model is clearly superior, providing an increase in the parameter precision by a factor of 1.5 to 10. These results can be rationalized as follows. With this moderate number of samples (51) in the time and wavelength domain the models were found to behave functionally (almost) linear [Figs. 2(c) and 3(c)]. Thus the covariance matrix of the parameters will be close to the inverse of the Fisher information matrix M [12]. Inspection of M (see the Appendix) shows that all elements of this matrix contain inner products $c_p^T c_q$ or $\varepsilon_p^T \varepsilon_q \, (p, q = 1, 2)$, as well as inner products with partial derivatives $\partial c / \partial \theta_K$ and $\partial \varepsilon / \partial \theta_S$. These inner products are a measure of the overlap of temporal or spectral properties, large inner products between different components being responsible for correlation, and imprecision of the parameters.

To study robustness against systematic deviations from the model assumptions data subject to time jitter, a common problem with time gated spectra [7], [8], were simulated. A uniformly distributed time jitter $(-0.05, 0.05)$ ns was simulated. Besides the kinetic and spectrotemporal model, also a spectral model of which the estimated concentration profiles were subsequently fitted with a kinetic model was used. It is clear from Table III that with low noise the last approach (column S; K) produces the most precise estimates

TABLE II
RMS DEVIATION OF RATE CONSTANTS (IN 10^6 s^{-1}) WITH KINETIC (K) OR SPECTROTEMPORAL (ST) MODEL AS A FUNCTION OF TEMPORAL AND SPECTRAL OVERLAP

		CS, ES		CL, ES		CS, EL		CL, EL	
	component	K	ST	K	ST	K	ST	K	ST
low noise	1	5	2	24	1	14	13	78	9
	2	11	7	26	3	19	18	77	18
high noise	1	43	24	240	20	150	130	2200	130
	2	110	73	340	170	290	200	1800	230

TABLE III
RMS DEVIATION OF RATE CONSTANTS (IN 10^6 s^{-1}) WITH CS, ES OVERLAP DATA SET AND TIME JITTER PRESENT USING A KINETIC (K), SPECTROTEMPORAL (ST) OR SPECTRAL FOLLOWED BY KINETIC (S;K) MODEL

	component	K	ST	S;K
low noise	1	10	4	3
	2	65	54	20
high noise	1	43	20	42
	2	110	76	620

of the parameters, thus confirming [8]. However, with high noise, the time jitter becomes relatively less important, and the spectrotemporal model is again superior.

The computational efficiency of the three types of models hardly depends upon the type of model, an iteration takes about 0.3 s on a midrange workstation. The number of iterations typically is less than five with proper initial values. With low noise levels the fit always converged to a global minimum. When choosing bad initial values in combination with high noise levels the spectrotemporal model performed better than the kinetic or spectral model, and local minima were most rare.

Finally, a model with three overlapping components has been investigated, namely the CS, ES pair from Table I augmented with a third component with parameters 0.5, 19, 9, 1 (first one of the CL, EL pair). With a low noise level ($\sigma = 6 \times 10^{-3}$ times the maximum of the data) it was not possible to resolve three components with the kinetic or spectral model, whereas the spectrotemporal model well recovered all parameters. Decreasing the noise down to $\sigma = 6 \times 10^{-5}$ the spectrotemporal model parameter precision was about ten times better than with the kinetic or spectral model.

IV. CONCLUSION

With a single component the parameter precision did not differ between the different model types, irrespective of the noise level used. With two or more components the precision decreases with a kinetic or spectral model because of overlap between concentration profiles or spectra of the components. However, with a spectrotemporal model the decrease is much less, and equals zero with zero spectral overlap (see the Appendix). This overlap is expressed as inner products of spectra or concentration profiles or derivatives thereof in the Fisher information matrix [see (A1), (A3), and (A4)]. Compared to a kinetic model, the improvement in precision using a spectrotemporal model is large when the spectral overlap is smaller than the temporal overlap (CL, ES case; see Figs. 2 and 3, and Table II). Compared to a spectral model the improvement is large when the temporal overlap is smaller than the spectral overlap.

When systematic errors are present, the choice of models should take these into account, e.g., with time jitter (a common problem with time-gated spectra) a spectral model is least sensitive to the amplitude fluctuations. With low-noise subsequent kinetic analysis of the thus estimated concentration profiles provides the best results. However, with high noise, the time jitter becomes relatively less important and the spectrotemporal model is superior again (Table III).

APPENDIX

The aim of this appendix is to compare the Fisher information matrix M for the kinetic and spectrotemporal model with two components. Using [17, Eq. (11)] it is found that with a kinetic model

$$M(k_1,k_2) = \sigma^{-2}\begin{bmatrix} \varepsilon_1^T\varepsilon_1 g_1^T P g_1 & \varepsilon_1^T\varepsilon_2 g_1^T P g_2 \\ \varepsilon_1^T\varepsilon_2 g_1^T P g_2 & \varepsilon_2^T\varepsilon_2 g_2^T P g_2 \end{bmatrix} \tag{A1}$$

where $g_l = dc_l/dk_l$ is an m-vector containing the derivative of the lth concentration vector with respect to the decay rate k_l, and $P = I - CC^\dagger$ is an orthogonal projection matrix of rank $m-2$ which projects on the space orthogonal to the column space of $C(k_1,k_2)$. Note in passing that with a single component the precision becomes independent of spectral shape (only $\varepsilon_1^T\varepsilon_1$ matters), thus confirming the result that with a single component model the precision of a kinetic model cannot be improved by a spectrotemporal model. When the spectra are orthogonal ($\varepsilon_1^T\varepsilon_2 = 0$) the estimates for the rate constants become uncorrelated. However, $g_1^T P g_1$ will be smaller than in the single component case, because of the overlap of the exponential decays. Thus even without spectral overlap the precision of the rate constants decreases when extra components are added.

The vector representation of the model function for the spectrotemporal model with two independently decaying components is

$$\sum_{l=1}^{2} a_l c_l(k_l) \otimes \varepsilon_l(\bar{\nu}_{\max,l}, \Delta\bar{\nu}_l) \tag{A2}$$

where $c_l \otimes \varepsilon_l$ denotes a Kronecker product, resulting in an mn-vector. Analogous to the derivation of (A1) in [17] it can be shown that the Fisher information matrix consists of four blocks

$$M(\theta) = \sigma^{-2}\begin{bmatrix} M_{11} & M_{12} \\ M_{21} & M_{22} \end{bmatrix} \tag{A3}$$

where $\theta = (k_1, a_1, \bar{\nu}_{\max,1}, \Delta\bar{\nu}_1, k_2, a_2, \bar{\nu}_{\max,2}, \Delta\bar{\nu}_2)^T$, and (see (A4), shown at the bottom of the page) where $f_l = \partial\varepsilon_l/\partial\bar{\nu}_{\max,l}$ and $h_l = \partial\varepsilon_l/\partial\Delta\bar{\nu}_l$ are n-vectors containing the partial derivatives of the lth spectrum vector with respect to the location and width parameters. Now consider

$$M_{pq} = \begin{bmatrix} a_p a_q g_p^T g_q \varepsilon_p^T\varepsilon_q & a_p g_p^T c_q \varepsilon_p^T\varepsilon_q & a_p a_q g_p^T c_q \varepsilon_p^T f_q & a_p a_q g_p^T c_q \varepsilon_p^T h_q \\ a_q c_p^T g_q \varepsilon_p^T\varepsilon_q & c_p^T c_q \varepsilon_p^T\varepsilon_q & a_q c_p^T c_q \varepsilon_p^T f_q & a_q c_p^T c_q \varepsilon_p^T h_q \\ a_p a_q c_p^T g_q f_p^T\varepsilon_q & a_p c_p^T c_q f_p^T\varepsilon_q & a_p a_q c_p^T c_q f_p^T f_q & a_p a_q c_p^T c_q f_p^T h_q \\ a_p a_q c_p^T g_q h_p^T\varepsilon_q & a_p c_p^T c_q h_p^T\varepsilon_q & a_p a_q c_p^T c_q h_p^T f_q & a_p a_q c_p^T c_q h_p^T h_q \end{bmatrix} \tag{A4}$$

again the case when there is no spectral overlap ($\varepsilon_1^T\varepsilon_2$, $\varepsilon_1^T f_2$, $\varepsilon_1^T h_2, f_1^T\varepsilon_2$, $h_1^T\varepsilon_2$ zero), then the estimates for the rate constants become again uncorrelated [$M_{12} = M_{21} = 0$ in (A3)]. In this case M_{11} in (A3) is equal to the single component case, and the precision is thus greater than with the kinetic model. With both types of model spectral overlap introduces correlation and thus worsens the precision.

ACKNOWLEDGMENT

The author would like to that Dr. H. J. W. Spoelder for critical reading of the text. The constructive comments of two reviewers helped to improve the manuscript.

REFERENCES

[1] J. M. Beechem, E. Gratton, M. Ameloot, J. R. Knutson, and L. Brand, "The global analysis of fluorescence decay data: Second generation theory and programs," in *Fluorescence Spectroscopy: Principles*, J. R. Lakowicz, Ed. New York: Plenum, 1992, vol. 2, pp. 241–305.

[2] N. Boens, L. D. Janssens, and F. C. de Schryver, "Simultaneous analysis of single-photon timing data for the one step determination of activation energies, frequency factors and quenching rate constants. Application to tryptophan photophysics," *Biophys. Chem.*, vol. 33, pp. 77–90, 1989.

[3] W. D. Hoff, I. H. M. van Stokkum, H. J. van Ramesdonk, M. E. van Brederode, A. M. Brouwer, J. C. Fitch, T. E. Meyer, R. van Grondelle, and K. J. Hellingwerf, "Measurement and global analysis of the absorbance changes in the photocycle of the photoactive yellow protein from *Ectothiorhodospira halophila*," *Biophys. J.*, vol. 67, pp. 1691–1705, 1994.

[4] A. R. Holzwarth, "Data analysis of time-resolved measurements," in *Biophysical Techniques in Photosynthesis*, J. Amesz and A. J. Hoff, Eds. Dordrecht, The Netherlands: Kluwer, 1996, pp. 75–92.

[5] J. R. Knutson, J. M. Beechem, and L. Brand, "Simultaneous analysis of multiple fluorescence decay curves: A global approach," *Chem. Phys. Lett.*, vol. 102, pp. 501–507, 1983.

[6] K.-H. Müller and Th. Plesser, "Variance reduction by simultaneous multi-exponential analysis of data sets from different experiments," *Eur. Biophys. J.*, vol. 19, pp. 231–240, 1991.

[7] I. H. M. van Stokkum, A. M. Brouwer, H. J. van Ramesdonk, and T. Scherer, "Multiresponse parameter estimation and compartmental analysis of time resolved fluorescence spectra," in *Proc. Kon. Ned. Akad. v. Wetensch.*, 1993, vol. 96, pp. 43–68.

[8] I. H. M. van Stokkum, T. Scherer, A. M. Brouwer, and J. W. Verhoeven, "Conformational dynamics of flexibly and semirigidly bridged electron donor-acceptor systems as revealed by spectrotemporal parameterization of fluorescence," *J. Phys. Chem.*, vol. 98, pp. 852–866, 1994.

[9] D. M. Bates and D. G. Watts, *Nonlinear Regression Analysis and Its Applications*. New York: Wiley, 1988.

[10] G. H. Golub and R. J. LeVeque, "Extensions and uses of the variable projection algorithm for solving nonlinear least squares problems," in *Proc. 1979 Army Numerical AnalysisComp. Conf., ARO Rep. 79-3*, 1979, pp. 1–12.

[11] L. Kaufman, "A variable projection method for solving separable nonlinear least squares problems," *BIT*, vol. 15, pp. 49–57, 1975.

[12] G. A. F. Seber and C. J. Wild, *Nonlinear Regression*. New York: Wiley, 1989.

[13] I. H. M. van Stokkum, "Solving a separable nonlinear least squares problem: Parameter estimation of time resolved spectra," *IMSL Directions*, vol. 9, no. 1, pp. 10–11, 1992.

[14] International Mathematical and Statistical Libraries, Houston TX, routines DRNLIN, DLQRSL.

[15] *Splus Reference Manual*, Statistical Sciences Inc., Seattle, WA, 1991.

[16] I. Brooks, D. G. Watts, K. K. Soneson, and P. Hensley, "Determining confidence intervals for parameters derived from analysis of equilibrium analytical ultracentrifugation data," *Meth. Enzymol.*, vol. 240, pp. 459–478, 1994.

[17] R. Pribić, I. H. M. van Stokkum, and A. van den Bos, "Inference regions of nonlinear parameters in global analysis," in *Proc. SYSID'94 10th IFAC Symp. System Identification*, M. Blanke and T. Söderström, Eds. Copenhagen, Denmark: Danish Automation Soc., 1994, pp. 2.423–2.428.

Ivo H. M. van Stokkum was born in Boxmeer, The Netherlands, in 1962. He received the M.Sc. degree in physics in 1984 and the Ph.D. degree in 1989, both from the University of Nijmegen, The Netherlands.

He is with the Faculty of Physics and Astronomy of the Vrije Universiteit, Amsterdam, The Netherlands. His research interests are global analysis, modeling, parameter estimation, photobiophysics, and spectroscopy.